Journal Pre-proof

Downregulation of intestinal Mdr-1 in obese mice: impact on its barrier function and role of TNF-α receptor 1 signaling

María Manuela Barranco , Virginia Gabriela Perdomo , Felipe Zecchinati , Romina Manarin , Greta Massuh , Nicolás Sigal , Silvana Vignaduzzo , Aldo Domingo Mottino , Silvina Stella Maris Villanueva , Fabiana García

PII: S0899-9007(23)00080-1
DOI: https://doi.org/10.1016/j.nut.2023.112050
Reference: NUT 112050

To appear in: *Nutrition*

Received date: 22 December 2021
Revised date: 17 March 2023
Accepted date: 22 March 2023

Please cite this article as: María Manuela Barranco , Virginia Gabriela Perdomo , Felipe Zecchinati , Romina Manarin , Greta Massuh , Nicolás Sigal , Silvana Vignaduzzo , Aldo Domingo Mottino , Silvina Stella Maris Villanueva , Fabiana García , Downregulation of intestinal Mdr-1 in obese mice: impact on its barrier function and role of TNF-α receptor 1 signaling, *Nutrition* (2023), doi: https://doi.org/10.1016/j.nut.2023.112050

HIGHLIGHTS

- High-fat diet induces downregulation of intestinal Mdr-1.
- High-fat diet-induced Mdr-1downregulation negatively impacts on its barrier function.
- TNF-α signaling plays a role in Mdr-1downregulation induced by high-fat diet.
- Impairment of the Mdr-1 barrier function may have consequences on drug bioavailability.

Downregulation of intestinal Mdr-1 in obese mice: impact on its barrier function and role of TNF-α receptor 1 signaling

María Manuela Barranco[a,b], Virginia Gabriela Perdomo[b,c], Felipe Zecchinati[d], Romina Manarin[c], Greta Massuh[a], Nicolás Sigal[a], Silvana Vignaduzzo[e], Aldo Domingo Mottino[d], Silvina Stella Maris Villanueva[d,#], Fabiana García[a,b, #]

[a]Laboratorio de Fisiología Metabólica, Facultad de Ciencias Médicas, Universidad Nacional de Rosario. Rosario, Santa Fe, Argentina.

[b]CONICET. Rosario, Santa Fe, Argentina.

[c]Área Parasitología, Facultad de Ciencias Bioquímicas y Farmacéuticas, Universidad Nacional de Rosario. Rosario, Santa Fe, Argentina.

[d]Instituto de Fisiología Experimental-CONICET. Rosario, Santa Fe, Argentina.

[e]Área Análisis de Medicamentos, Facultad de Ciencias Bioquímicas y Farmacéuticas, Universidad Nacional de Rosario. Rosario, Santa Fe, Argentina.

[#]Contributed equally and are co-senior authors

Corresponding author:
Fabiana García, Ph.D.
Laboratorio de Fisiología Metabólica. CONICET-Rosario. Facultad de Ciencias Médicas (UNR).
Santa Fe 3102.
(2000) Rosario. Argentina.
Phone: 54-9-341-6096749

E-mail: fgarcia@fmedic.unr.edu.ar

ABSTRACT

Multidrug resistance transporter-1 (Mdr-1) is a relevant component of the intestinal transcellular barrier by decreasing oral drugs absorption, thus modulating their bioavailability. Obese patients with metabolic disorders take medicaments that are subjected to intestinal metabolism and Mdr-1-dependent barrier.

Objective: Evaluate the effect of a high-fat diet (HFD, 40% fat for 16 weeks) on Mdr-1 expression and transport activity, in C57BL/6 (C57) male mice. Comparable studies were performed in TNF-α receptor 1 knockout mice (R1KO) to delineate a possible role of TNF-α signaling. Methods: mRNA expression was evaluated by real-time PCR, and protein levels by western blotting and immunohistochemistry. Mdr-1 activity was assessed using the everted intestinal sac model, with Rhodamine 123 as substrate. Statistical comparisons: student-t test or one-way ANOVA followed by the post hoc Tukey test.

Results: Mdr-1 protein as well as its corresponding mRNAs *Mdr1a* and *Mdr1b* was decreased in C57-HFD compared with controls. Immunohistochemical studies confirmed downregulation of Mdr-1 *in situ*. These results correlated with a 48% decrease in the basolateral to apical transport of Rhodamine 123. In contrast, R1KO-HFD neither modified intestinal Mdr-1 mRNAs, nor its protein expression or activity. Besides, C57-HFD showed elevated intestinal TNF-α mRNA and protein (ELISA assay) levels, whereas in R1KO-HFD was undetectable or either with lower increase, respectively.

Conclusion: We demonstrate for the first time an impairment of the Mdr-1 intestinal barrier function induced by HFD as a consequence of both *Mdr-1* gene homologues downregulation, resulting in impaired Mdr-1 protein expression. TNF-α receptor 1 signaling-mediated inflammatory response is likely involved.

Keywords: high-fat diet; Mdr-1; inflammation; TNFR1.

Abbreviations:

ABC, ATP-binding cassette; AUC, area under the curve; BBM, brush border membrane; C, control; ELISA, Enzyme-Linked Immunosorbent Assay; HFD, High-fat diet; IPGTT, intraperitoneal glucose tolerance test; ITT, intraperitoneal insulin tolerance test; MetS, metabolic syndrome; Mdr-1, Multidrug resistance transporter-1; TNF-α, Tumor necrosis factor-alpha; TNFR1, Tumor necrosis factor receptor 1; R1KO, Tumor necrosis factor receptor 1 knockout; w/v; weight/volume; P-gp, P-glycoprotein; CYP3A, cytochrome P450 3A; R123, Rhodamine 123.

INTRODUCTION

Multidrug resistance transporter 1 (Mdr-1, AbcB1), also termed P-glycoprotein (P-gp), is an efflux drug transporter belonging to the ATP-binding cassette (ABC) family. It is expressed in many tissues including liver, intestine, kidney and brain among others. In particular, in intestine, Mdr-1 is found in the apical membrane of enterocytes predominantly at the ileum level [1, 2]. Mdr-1, working in concert with the biotransformation enzyme cytochrome P450 3A (CYP3A), constitutes a major component of the intestinal transcellular barrier by decreasing the absorption of dietary contaminants and additives as well as therapeutic drugs orally incorporated, therefore limiting their oral bioavailability [3, 4]. Mdr-1 expression and/or activity can be regulated under certain pathological processes such as metabolic syndrome (MetS) or diabetes [5, 6].

Solid evidence indicates that obesity is the driving force behind the MetS development [7]. Noticeably, the obesity is a pathological condition that occurs with chronic systemic inflammation, linked to over nutrition and constituting a precursor factor to a number of co-morbidities, with the metabolic disease being the most prominent [8, 9].

Of particular interest is the fact that metabolic disorders are also a risk factor for drug toxicity, since patients under these conditions take medicaments that require intestinal metabolism and transport, and frequently exhibit variations in their bioavailability [10]. Consequently, it is important to determine whether changes in the intestinal Mdr-1 function occur in such conditions, which could result in altered therapeutic efficiency or eventually increased toxicity of Mdr-1 substrates of medicinal use.

Feeding mice with a high-fat diet (HFD) can induce metabolic disorders resembling the human pathology. In this condition, it is induced the production of proinflammatory

mediators, such as tumor necrosis factor-alpha (TNF-α), interleukin-1 beta (IL-1β) and interleukin-6 (IL-6) [11].

TNF-α is the first proinflammatory cytokine described in adipose tissue linking insulin resistance to obesity [12]. On this regard, it has been reported an increased expression of TNF-α in obese mice and humans [13] and its neutralization reverts insulin resistance in rodents [12]. Particularly in the case of the intestine, it has been shown that mice fed with HFD promote TNF-pathway activation in ileal epithelial cells [14].

TNF-α signal transduction is mediated by two main transmembrane receptors, Tumor necrosis factor receptor 1 (TNFR1) expressed in all cell types and Tumor necrosis factor receptor 2 restricted to immune cells, endothelial cells and neurons [15]. Several reports used TNFR1 knockout (R1KO) mice as a model to delineate the role of TNFR1 mediated TNF-α signaling in certain pathophysiological situations [16, 17].

The impact of obesity on intestinal Mdr-1 expression and activity has been poorly explored. This is a subject of relevance considering that many drugs of therapeutic use are substrates of Mdr-1 and at the same time are subjected to first-pass metabolism at the intestinal level. Indeed, only two reports are available in the literature studying the effect of obesity models in mice, and present opposite results on Mdr-1 expression [18, 19], whereas none of them explored functional aspects of this transporter. In contrast, regulation of expression and/or activity of ABC transporters by proinflammatory mediators eventually associated to obesity, have been largely characterized [20, 21]. Concerning Mdr-1 regulation by TNF-α, it has been reported in *in vitro* studies, in human hepatoma cells and primary trophoblast cells, downregulation of Mdr-1 mRNA and protein levels as well as in its functionality [22, 23].

However, to what extent TNF-α affects Mdr-1 expression and activity in the context of obesity and which particular type of TNF-α receptor is involved remain unknown.

Therefore, the aim of our study was to evaluate the expression and activity of intestinal Mdr-1 in mice developing a model of obesity by feeding HFD for 16 weeks. Studies were also performed in R1KO mice in order to ascertain the particular influence of TNF-α receptor 1 signaling under the current obesity conditions.

MATERIALS AND METHODS

Chemicals. Rhodamine 123 was obtained from Sigma-Aldrich (St. Louis, USA). PSC833 was purchased from Santa Cruz Biotechnology (Dallas, Texas, USA). All other chemicals and reagents used were commercial products of analytical-grade purity.

Animals and treatments. Young male C57BL/6 mice (20-25 g body weight, 5 weeks old, n= 20/group) were purchased from Centro de Investigación y Producción de Reactivos Biológicos (CIPReB), School of Medicine, National University of Rosario. Knockout C57BL/6-Tnfrsf1atm1Imx/J (R1KO) mice (20-25 g body weight, 5 weeks old, n= 20/group), originally obtained from The Jackson Laboratory, were gently provided by Dr. Silvia Di Genaro. C57BL/6 and R1KO animals received *ad libitum* tap water and either standard commercial diet (C57-C and R1KO-C groups) or standard commercial diet enriched with 40% of fat (C57-HFD and R1KO-HFD groups), for 16 weeks to induce obesity [24, 25, 17]. Mouse chow was purchased from GEPSA (http://www.gepsa.com) and the 40% high-fat diet was prepared as in Lambertucci et al. [17]. Animals were grouped (five animals per cage) and kept under controlled conditions (23 ± 2°C) with a fixed 12 h light-dark cycle (07:00-19:00). At the beginning of the treatment, animals from all experimental groups were subjected to an Intraperitoneal Glucose Tolerance Test (IPGTT) to assess basal glycemic metabolism as described previously Londero et al. [26]. Body weight (g) and calories intake (kcal/animal) were measured weekly. Body weight gain is expressed as percentage (final weight x 100/initial weight).

One week before the end of the treatments, development of insulin resistance was confirmed by an Intraperitoneal Insulin Tolerance Test (ITT). All the experimental protocols were performed according to the Regulation for the Care and Use of Laboratory Animals and were approved by the Institutional Animal Use Committee of the National University of Rosario, Argentina (Expedient 6109/012 E.C. Resolution 267/02).

Specimen collection. Animals were fasted for 12 h and anesthetized (ketamine 200 mg/kg-midazolam 5 mg/kg body weight). After an abdominal incision, blood samples were obtained by cardiac puncture and placed into heparinized tubes to measure plasmatic levels of glucose, triacylglycerol and total cholesterol. Fats pads were removed from epididymal deposits and wet mass were determined and expressed as % of final body weight (epididymal fat weight x 100/ final body weight). For collection of ileum specimens, the entire small intestine was extracted (pyloric to ileocecal valve) and divided in 3 segments: the first two/thirds corresponding to duodenum and jejunum were excluded and the last third of approximately 10 cm was taken and considered as the ileum. This segment was carefully rinsed with ice-cold saline and dried with filter

paper. For total RNA isolation, small rings were cut from this same region of the intestine, frozen in liquid nitrogen and kept at -70°C until isolation for Real-Time Polymerase Chain Reaction (PCR) studies. For immunohistochemical studies, ileum small rings were fixed in formaldehyde buffer. For Western blot studies, the ileum was directly opened lengthwise, the mucus layer was carefully removed, and the mucosa was obtained by scraping, weighed, and used for brush border membrane (BBM) preparation. For Mdr-1 transport studies, segments of the ileum were immediately used in preparation of everted sacs. Aliquots of ileum were homogenized in ice-cold phosphate-buffered saline (pH: 7.40) (1:2) for measurement of TNF-α levels by specific two-site enzyme-linked immunosorbent assay (ELISA).

Biochemical assays. The IPGTT was performed before the animals were subjected to the dietary treatment, as described previously [26]. For the calculation of the area under the curve (AUC) the GraphPad Prism 7 software was used and the values were expressed in mg/dL/120 min.

Plasma glucose, triacylglycerol and cholesterol levels were determined spectrophotometrically using commercial kits (Wiener Laboratorios, Rosario, Argentina). The ITT was performed 5 days before animals were euthanized [27]. The values were expressed as maximum percentage decrease in blood glucose during the test [28, 29].

Histological assays. Epididymal fat pads were fixed in 4% buffered formalin, paraffin-embedded, sectioned and stained with hematoxylin-eosin (HE) stain and then visualized by optical microscopy (40X). Histological analysis of adipocytes was performed using ImageJ software. Adipocyte area was measured in at least 60 cells per mouse (n: 6-10 mice per group) and the presence of macrophage crown-like structure per field was evaluated [30].

Real-Time PCR studies. Total RNA was isolated from ileum samples using TRI Reagent, (Molecular Research Center Inc, Cincinnati, USA) according to manufacturer's instructions. Quality and quantity of RNA were evaluated through agarose gel electrophoresis and spectrophotometry (Abs 260nm/280nm), respectively [31]. Five micrograms of RNA were used in the RT reaction with oligo (dT) and the Omniscript kit (Qiagen, Inc.) according to manufacturer's instructions to obtain the cDNA. Real time PCR reactions were carried out on a StepOne (Applied Biosystem,

Thermo Fisher Scientific, Foster city, CA, USA) with Power SYBR Green PCR Master Mix (Solis Biodyne, Tartu, Estonia) using specific primers (Table 1) [32-34]. The efficiency of the real time PCR assays were ensuring by the use of positive controls for each evaluated gene.

Results for gene mRNAs were normalized to the Glyceraldehyde-3-phosphate dehydrogenase (GAPDH) mRNA as housekeeping gene [17]. The results were analyzed as relative quantification through the $2^{-\Delta\Delta CT}$ method and expressed as % of C57-C group [35].

The specificity of each reaction was verified with a melting curve between 55 ºC and 95 ºC with continuous fluorescence measure [34].

Table 1: Primers used for the analysis of mRNA expression

Gene	Gene Description	Primer Sequence
Mdr-1	*Mdr1a* [31]	Fw 5´-AAAGGCTCTACGACCCCCTA-3´
		Rv 5´-CCTGACTCACCACACCAATG-3´
	Mdr1b [32]	Fw 5´-TTGGTGGCACAACAACTCAT-3´
		Rv 5´-GGCTTTCGCATAGTCAGGAG-3´
TNF-α	*Tumor necrosis factor-α* [33]	Fw 5´-TGTGGCTTCGACCTCTACCTC-3´
		Rv 5´-GCCGAGAAAGGCTGCTTG-3´
GAPDH	*Glyceraldehyde-3-phosphate dehydrogenase* [16]	Fw 5´-CACAATTTCCATCCCAGACC-3´
		Rv 5´-GTGGGTGCAGCGAACTTTAT-3´

Immunohistochemical studies. Ileum fixed samples in 10% buffered formaldehyde, from all groups, were dehydrated and paraffin embedded. After deparaffinization of tissue sections in xylene, endogenous peroxidase activity was blocked with 3% H_2O_2. Thereafter, sections were incubated overnight at 4°C with the primary antibody (Mdr-1 (D-11): sc-55510, Santa Cruz Biotechnology, Dallas, Texas, USA). Then, the CytoScan HRP Detection System (Cell Marque, Sigma Aldrich, California, USA) was used. The polyvalent biotinylated link was applied and samples were incubated for 30 min at room temperature. The HRP streptavidin-label was added and incubated for 30 min. The Mdr-1 immunoreactivity was visualized with 3,3′-diaminobenzidine (DAB) staining (Sigma Aldrich, California, USA), according to the supplier's instructions. Finally, sections were counterstained with hematoxylin, dehydrated and cleared with xylene. Microphotographs were taken with a Nikon Eclipse CI-L microscope (Nikon

Corporation, Tokyo Japan) [36, 37]. Negative controls were performed to evaluate the specificity of the immunohistochemical test (images not shown).

Western blot studies. Mdr-1 was detected in BBMs as previously studied by Arana et al [38]. BBM were prepared from mucosa samples as described before [36]. Briefly, aliquots of the BBM preparations were kept on ice and used the same day in Western blot studies. Protein concentration was measured by using bovine serum albumin as standard [39]. Equal loading and transference of protein was systematically checked by both detection of β-actin and staining of the membranes with Ponceau S. Primary antibodies used were anti-Mdr1 (Mdr-1 (D-11): sc-55510, Santa Cruz Biotechnology, Dallas, Texas, USA) and anti-β-actin (A-2228, Sigma– Aldrich). Immunoreactive bands were quantified with Gel-Pro Analyzer software (Media Cybernetics, Inc., Bethesda, USA).

Assessment of Mdr-1 activity *in vitro*. To characterize the effect of the administration of a high-fat diet to mice on intestinal Mdr-1 efflux activity, the *in vitro* model of everted sacs was chosen, where Rhodamine 123 (R123) was used as substrate. In this model, R123 is added in the serosal compartment (inside the sac), and is pumped to the mucosal compartment (outside the sac) by Mdr-1 [40]. This measure well estimates the intestinal barrier function associated to Mdr-1. Briefly, segments from ileum were everted, filled with 20 μM R123 and incubated for 30 min with or without the addition of the Mdr-1 inhibitor PSC833 (10 μM). Samples of the mucosal compartment were obtained at the beginning and at the end of the incubation and subjected to fluorescence analysis (λex=485, λem=535) [38]. The results were expressed as % of C57-C group.

ELISA assay. Ileum homogenates were sonicated with an ultrasonifier [Sonics (Newtown, CT, USA) Vibra-cell VCX 130] by six cycles (20 s sonications and 40 s pause on ice). The sonicated was centrifuged at 15000 g, for 10 min at 4°C and the supernatants were subjected immediately to TNF-α measurement by ELISA technique according to the protocol provided by the manufacturer (BD opEIA, mouse TNF mono/mono ELISA set, BD Biosciences, San Diego, California, USA) [26].

Statistical analysis. Data are presented as mean ± standard error (S.E.). The statistical comparison of the results obtained in the different experimental groups were carried out using student-t test or one-way ANOVA followed by the post hoc Tukey test for

multiple comparisons. Differences were considered to be statistically significant from a value of $P<0.05$.

RESULTS

Verification of baseline glycemic metabolism in C57BL/6 and R1KO mice

Before starting the HFD dietary treatment, 6-week-old C57BL/6 and R1KO mice were subjected to IPGTT and exhibited a glycemic response with a maximum of 229.80 ± 24.74 mg/dL for C57BL/6 and 258.40 ± 8.25 mg/dL for R1KO mice at 30 min, and a progressive decrease to 102.90 ± 10.33 mg/dL and 113.30 ± 5.88 mg/dL at 120 min, respectively (Figure 1A). There were no significant differences in the IPGTT response between both strains of mice (Figure 1B).

Figure 1

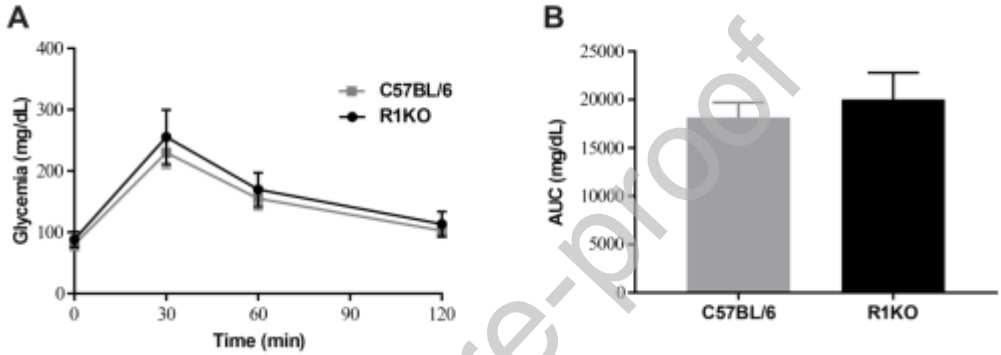

Figure 1: Intraperitoneal Glucose Tolerance Test (IPGTT). (A) Graph represents glycemic response to glucose overload within 120 minutes after injection. (B) Area under curve of IPGTT (mean ± S.E.), no statistical difference was found between C57BL/6 and R1KO mice.

Effect of HFD on physiological and biochemical parameters in C57BL/6 and R1KO mice: obesity model establishment

Table 2 shows that after HFD treatment, the calories consumed by R1KO mice were similar to the wild-type counterpart (C57-C). Both high fat-fed groups consumed more calories (C57-HFD: +36%; R1KO-HFD: +38%) than their respective control groups. Consequently, the HFD groups significantly increased their body weight (C57-HFD: +54%; R1KO-HFD: +45%) at the end of the feeding regimen compared to their respective controls. No difference in body weight gain was found between the KO and wild-type strains.

In both strains of mice, the high-fat feeding regime resulted in more adiposity with respect to controls, as shown by a significant increase in the weight of epididymal fat

panicles (C57-HFD: +154%; R1KO-HFD: +158%). Moreover, no difference was found between the KO and wild-type strains in this parameter.

In agreement with previous reports [24, 25, 17], the present study shows in Table 2, that after feeding male C57BL/6 mice with HFD during a 16-week period, they exhibited increased glycemia and features of insulin resistance as well as greater triglyceridemia and cholesterolemia when compared to control animals. In contrast to what was observed for wild-type animals, and in line with previous studies [41], R1KO-HFD mice did not show elevated glycemia levels or insulin resistance. Regarding lipid metabolism, R1KO-HFD mice showed increased triglyceridemia and cholesterolemia levels than their respective controls (Table 2).

We then examined histological preparations of epididymal adipose tissue from C57BL/6 and R1KO mice. As expected and irrespective of the strain, mice fed with HFD significantly increases in the adipocyte size with respect to their controls (C57-HFD: +72%; R1KO-HFD: +66%). However, KO animals showed smaller sizes (R1KO-C: 35.7 ± 0.7; R1KO-HFD: 59.3 ± 0.9 µm) than the C57BL/6 mice (C57-C: 41.7 ± 1 C57-HFD: 71.6 ± 15.8 µm) (Figure 2B). C57-HFD fed mice showed macrophages infiltration, visualized as crown-like structures around adipocytes that were not found in R1KO-HFD mice (Figure 2A).

Table 2: Effect of HFD on morphometric and biochemical parameters of C57BL/6 and R1KO mice

Obesity features	**C57-C**	**C57-HFD**	**R1KO-C**	**R1KO-HFD**
Calories intake (kcal total/animal)	1293 ± 42.92	1760 ± 43.45$^{\&\#}$	1396 ± 76.65	1921 ± 20.54$^{\&\#}$
Body weight gain (%)	41.55 ± 2.47	63.84 ±3.66$^{\&\#}$	43.46 ±3.56	62.86 ±2.36$^{\&\#}$
Epididymal fat (%)	1.09 ± 0.18	2.77 ± 0.15$^{\&\#}$	0.96 ± 0.09	2.48 ± 0.20$^{\&\#}$
ITT (%)	34.38 ± 12.71	19.12 ± 9.86$^{\&\#\dagger}$	37.33 ± 6.41	34.76 ±17.55
Glycemia (mg/dL)	73.90 ± 6.10	98.10 ± 13.03$^{\&\#\dagger}$	76.20 ± 4.15	71.25 ± 8.24
Cholesterolemia (mg/dL)	89.14 ± 12.91	199.40 ± 25.15$^{\&\#\dagger}$	89.58 ± 7.84	119.60 ± 7.97$^{\&\#}$
Triglyceridemia (mg/dL)	71.78 ± 26.58	121.30 ± 21.14$^{\&\#}$	74.16 ± 14.80	118.50 ± 13.55$^{\&\#}$

Data are shown as mean ± S.E. Body weight gain: final weight x 100/initial weight. The amount of epididymal fat was calculated as: epididymal fat weight x 100 / final body weight. ITT is expressed as maximal percentage of the decrease in blood glucose during the test. [&], significantly different from C57-C, $P<0.05$. [#], significantly different from R1KO-C, $P<0.05$. [†], significantly different from R1KO-HFD, $P<0.05$.

Figure 2

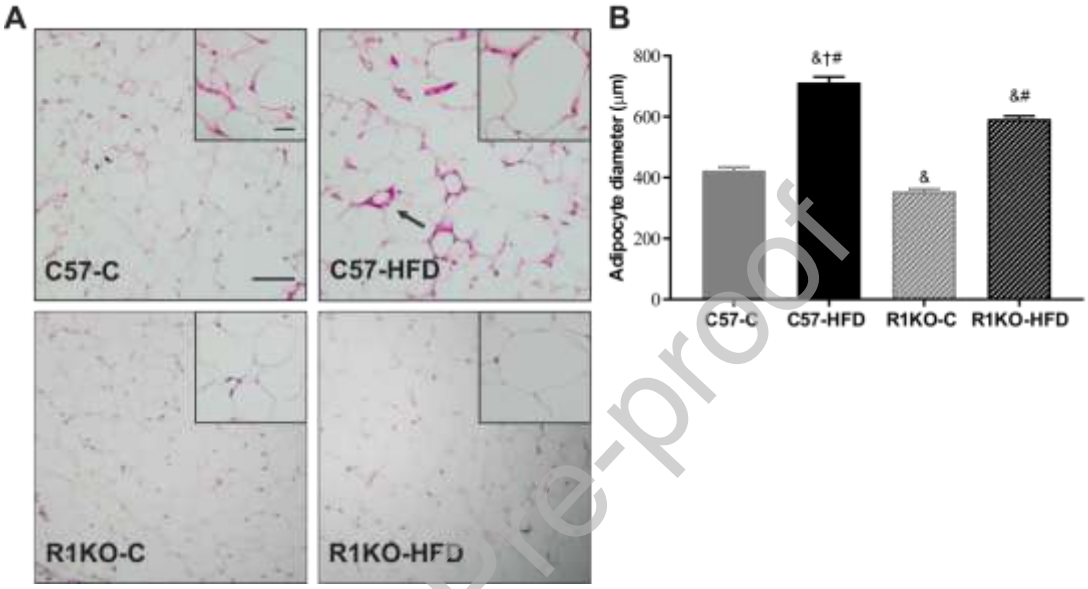

Figure 2: Histological analysis in HE-stained adipose tissue of C57BL/6 and R1KO mice. (A) Images are shown at 10X magnification (bar indicates 100 μm), the areas selected in the insets are at 40X magnification (bar indicates 50 μm). A representative macrophage crown-like structure is marked with the arrow. (B) Adipocyte diameter (mean ± S.E.). [&], significantly different from C57-C, $P<0.05$. [#], significantly different from R1KO-C, $P<0.05$. [†], significantly different from R1KO-HFD, $P<0.05$.

Effect of HFD on Mdr-1 expression and activity

Next, we evaluated the expression and transport activity of Mdr-1 in the ileum of C57BL/6 and R1KO mice after HFD feeding. In C57BL/6 mice, HFD caused a 71% decrease of Mdr-1 protein expression (Table 3; Figure 3A). Although we did not perform a quantitative analysis of the immunohistochemical images, we observed that detection of Mdr-1 at the surface of the microvilli was weaker in C57-HFD fed mice when compared to controls (Figure 3B). This contrast was consistently observed in all the images available and is in well correlation with data on proteins expression. Furthermore, HFD caused a 62% decrease in expression of *Mdr1a* mRNA and a 66%

decrease in expression of *Mdr1b* mRNA (Table 3; Figure 3C, 3D), suggesting participation of a transcriptional mechanism. As a significant contribution of our study, HFD did not modify Mdr-1 protein expression or its expression at the surface of the microvilli as detected *in situ* and neither changed intestinal *Mdr1a* or *Mdr1b* mRNAs expression in R1KO mice (Table 3; Figure 3A, 3B, 3C, 3D).

Consistent with the data on Mdr-1 expression, the amount of R123 accumulated in the mucosal compartment of the everted intestinal sacs was significantly lower in C57-HFD group (-55%) than in C57-C (Table 3; Figure 3E). This result is consistent with a lower intestinal Mdr-1 mediated efflux of the R123. Importantly, Mdr-1 activity was not altered in R1KO mice after 16 weeks of HFD feeding in well agreement with the unaffected levels of protein and mRNAs (Table 3; Figure 3E).

Figure 3F shows that the ileum from C57 groups exhibited a decrease in R123 apical accumulation after addition of Mdr-1 inhibitor, thus confirming participation of this transporter in the current findings.

Table 3: Effect of HFD on Mdr-1 expression and activity

	Mdr-1 protein expression (%)	**mRNA expression**		**Activity of Mdr-1 (%)**
		Mdr1a (%)	***Mdr1b (%)***	
C57-C	100.00 ± 4.01	100.00 ± 21.24	100.00 ± 35.01	100.00 ± 11.57
C57-HFD	28.64 ± 0.27$^{\&\#\dagger}$	38.21 ± 14.35$^{\&\#\dagger}$	34.14 ± 11.23$^{\&\#\dagger}$	45.44 ± 7.38$^{\&\#\dagger}$
R1KO-C	89.93 ± 4.98	80.29 ± 12.79	116.10 ± 20.60	78.74 ± 7.45
RIKO-HFD	83.14 ± 7.64	75.61 ± 5.56	106.90 ± 23.41	85.52 ± 9.59

Data are calculated as % of C57-C and shown as mean ± S.E. Mdr-1 activity in everted sacs using R123 as substrate. $^{\&}$, significantly different from C57-C, $P<0.05$. $^{\#}$, significantly different from R1KO-C, $P<0.05$. †, significantly different from R1KO-HFD, $P<0.05$.

Figure 3

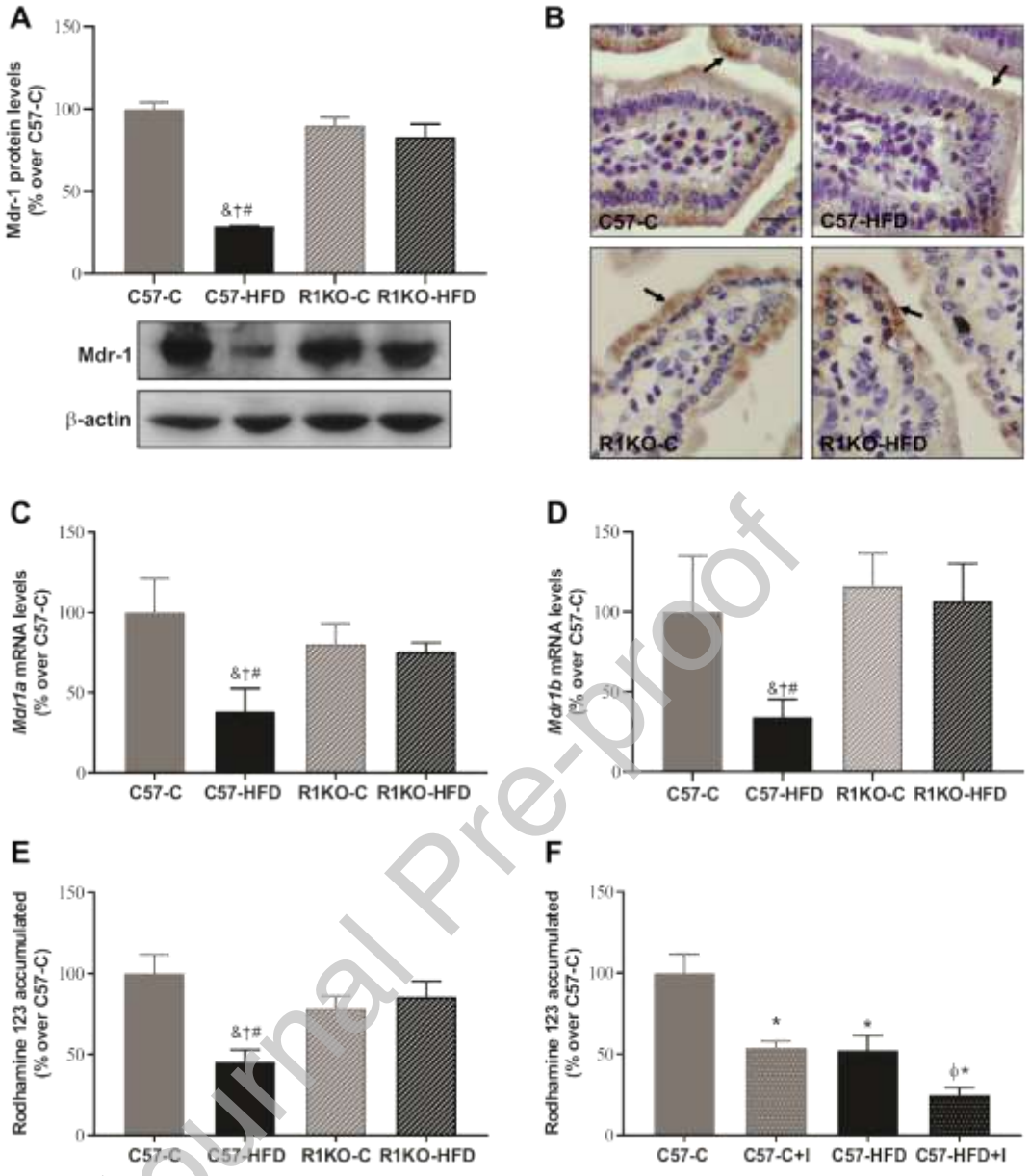

Figure 3: Effect of HFD on expression and activity of intestinal Mdr-1 in C57BL/6 and R1KO mice. Data are shown as mean ± S.E. (A) Mdr-1 protein levels. (B) Representative images of Mdr-1 expression as detected *in situ*. Positive immunostaining is observed in C57-C, R1KO-C and R1KO-HFD and marked with black arrows, whereas a much weaker signal is detected in C57-HFD (black arrow). Bar indicates 100 µm. (C) *Mdr1a* mRNA levels. (D) *Mdr1b* mRNA levels. (E) Mdr-1 activity in everted sacs using R123 as substrate. Graphic shows R123 accumulation at 30 min. $^{\&}$, significantly different from C57-C, $P<0.05$. $^{\#}$, significantly different from R1KO-C, $P<0.05$. †, significantly different from R1KO-HFD, $P<0.05$. (F) Mdr-1 activity with addition of the Mdr-1 inhibitor PSC833. (C57-C+I and C57-HFD+I) or without (C57-C

and C57-HFD) *, significantly different from C57-C, $P<0.01$. $^{\phi}$, significantly different from C57-HFD, $P<0.05$.

Intestinal TNF-α expression

We determined TNF-α protein levels in the same intestinal region used in Mdr-1 studies. We observed that C57-HFD group showed a significant increase (+65%) when compared to C57-C. R1KO-C showed practically complete suppression of this cytokine, compared with C57-C mice fed with standard diet. R1KO-HFD showed an increment of TNF-α in intestinal tissue; however, its level was still lower than C57-HFD (Table 4, Figure 4 A).

Additionally we measured TNF-α mRNA levels in ileum tissue. C57-HFD group showed a significant increase of this proinflammatory cytokine (+148%) when compared to the respective controls (Table 4, Figure 4B). In contrast, TNF-α mRNA expression, was below the assay detection level, in ileum homogenates from R1KO mice irrespective of whether they were fed with HFD or not.

Table 4: Effect of HFD on intestinal TNF-α protein and messenger RNA levels

	C57-C	C57-HFD	R1KO-C	R1KO-HFD
TNF-α protein levels	100 ± 16.92	165 ± 13.34$^{\&\#}$	ND	42.37 ± 9.69$^{\&}$
TNF-α mRNA levels	100 ± 6.53	248 ± 44.45$^{\&}$	ND	ND

Data are calculated as % of C57-C and shown as mean ± S.E. $^{\&}$, significantly different from C57-C, $P<0.05$. †, significantly different from R1KO-HFD, $P<0.05$. ND: non detectable.

Figure 4

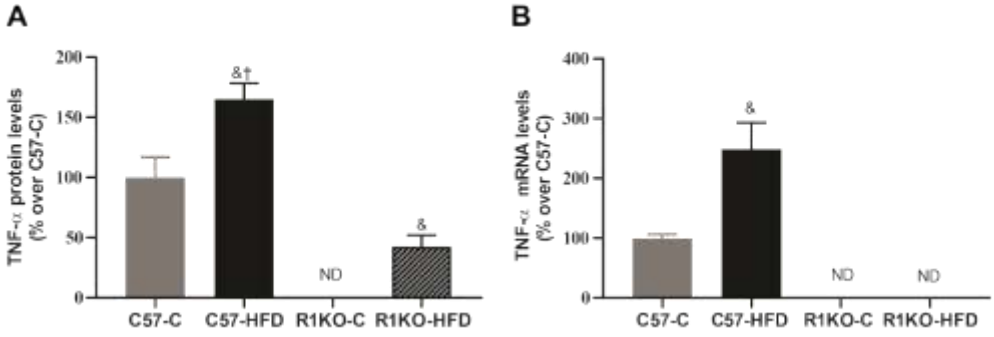

Figure 4: Effect of HFD on intestinal TNF-α expression in C57BL/6 and R1KO mice. Data are shown as mean ± S.E. (A) TNF-α protein levels. (B) TNF-α mRNA levels. [&], significantly different from C57-C, $P<0.05$. [†], significantly different from R1KO-HFD. ND: non detectable.

DISCUSSION

Over the last decades, the incidence of obesity has risen dramatically to the extent that it is considered a global epidemic. Experimental models mimicking this pathology represent a valuable tool to explore potential strategies to prevent or, better yet, revert its consequences. Our data confirm that in mice under HFD, the obesity model is successfully established. In addition, mice lacking TNFR1, which disrupts TNF-α signaling, exhibited sings of obesity as visualized by dyslipidemia and large epididymal fat mass, but preserved the systemic sensitivity to insulin, in response to HFD. This latter data are in line with those from Bhering Martins and colleagues demonstrating that ablation of TNFR1 in mice protected from insulin resistance induced by a high carbohydrate diet for 16 weeks [41].

The function of the intestinal transcellular barrier is conditioned by a complex array of enzymes and transport proteins present in the enterocyte, which metabolize and excrete compounds back to the gut lumen. One of the relevant transporters that regulate this barrier function is the efflux transporter Mdr-1, which reduces the absorption and systemic distribution of a large amount of xenobiotics, such as therapeutic drugs incorporated via the gastrointestinal tract [42]. Significantly, the present study shows that HFD treatment reduced Mdr-1 protein expression along with *in situ* protein levels, as well as the expression of intestinal *Mdr1a* and *Mdr1b* mRNA, in well correlation with a lower transport rate of R123, a recognized Mdr-1 substrate. Even more, the participation of Mdr-1 in R123 transport was confirmed by inhibition with PSC833, a known inhibitor of the transporter. Interestingly, it was shown that expression of intestinal CYP3A, an important biotransformation enzyme working in concert with Mdr-1, is also diminished in an obesity model [43]. Taken together, the data suggest altered disposition of compounds requiring sequential action of both systems. This may involve compounds of therapeutic use, eventually leading to alterations in their bioavailability and safety.

So far, previous investigations focused on the study of Mdr-1 expression in metabolic diseases. One of them showed a decrease in intestinal Mdr-1 protein and mRNA

expression after a 24-week period of HFD feeding with respect to control mice [19]. In a second study, the authors found lower expression of intestinal Mdr-1 in Type 1 diabetes induced by streptozotocin in mice [44]. On the contrary, in a model of obesity induced by injection of monosodium glutamate at birth, Mdr-1 protein expression was increased in jejunum [18]. Our study supports the preliminary study by Lu et al. [19] and, more importantly, demonstrated for the first time an impairment of Mdr-1 functionality, which resulted in loss of 50% of the native activity.

As a major contribution of our study, we explored the biological significance of abolishing the signaling and function of TNFR1 on intestinal Mdr-1 expression and activity in the context of obesity conditions. Our results show that the administration of HFD to R1KO mice did not affect the expression or the activity of intestinal Mdr-1 as indeed occurred in wild-type mice (see Figure 3). Consequently, it is reasonable to speculate that TNF-α acting on type 1 receptor constitutes a relevant pathway in Mdr-1 regulation in our model. In support to this conclusion, a previous study showed a direct effect of TNF-α in Caco-2 cells, which resulted in decreased MDR-1 expression at mRNA level as well as in its efflux activity [45]. In line with this, another study in colorectal carcinoma cells showed that TNFR1 is essential to reduced NF-κB signaling leading to ABCB1 downregulation after long-term TNF-α treatment [46]. Our results showed that under high fat diet treatment, TNF-α mRNA was not detected in intestinal tissue from knockout mice, besides, TNF-α protein levels was lower in R1KO-HFD respect to C57-HFD. In these sense and in accordance with our observations, one study reported that high carbohydrate-fed mice with ablated TNFR1 results in lower content of inflammatory cytokines among them, TNF-α, in adipose tissue [41]. Herein, although the TNF-α protein was detected in the intestinal tissue of the R1KO-HFD mice, possibly due to the infiltration of inflammatory cells, since the TNFR1 pathway is inactive in the knockout mice, it could confirm that the TNF-α signaling pathway is required for Mdr-1 negative regulation. Indeed, TNFR1 seems to be the prevalent type receptor in intestinal tissue in different species including mice [47]. Collectively, it is clear that it is the TNF-α-TNFR1 pathway which is involved in regulating Mdr-1 in intestine from wild-type animals subjected to HFD.

The lack of appearance of proinflammatory milieu in adipose tissue in response to knocking down TNFR1, as shown in Figure 2, is consistent with the concept that the TNF-α-TNFR1 pathway is indeed inactive in these animals [41].

Finally, because other proinflammatory cytokines are released under obesity conditions, either in patients or animal models like the one currently used, we cannot rule out that they contribute, together with TNF-α, to Mdr-1 downregulation and to the consequent alteration of the associated transcellular barrier function. Further studies are necessary to clarify this issue.

CONCLUSION

Herein, our main findings are: i) The obesity and consequent metabolic alterations induced a decrease in intestinal Mdr-1 (P-gp) expression, with significant impact on its efflux activity. ii) The TNF-α-TNFR1 pathway is, at least in part, responsible for the reduction of the expression and transport activity of intestinal Mdr-1. Our data alert on the potential impact on intestinal first-pass metabolism of drugs associated to Mdr-1 under conditions of obesity, with eventually occurrence of overdose effects.

ACKNOWLEDGMENTS

We express our gratitude to Dr. Marcelo G. Luquita and Htl Diego Parenti for their invaluable technical assistance.

Funding: This study was supported by grants from: Consejo Nacional de Investigaciones Científicas y Técnicas (CONICET) [PIP 2017-1112] (to F.G.), Fondo para la Investigación Científica y Tecnológica (FONCyT) [PICT 2018-01059 (to S.S.M.V.) and PICT 2017-1098 (to A.D.M.)].

Conflict of interest: The authors declare no competing financial interests

REFERENCES

[1] Zimmermann C, Gutmann H, Hruz P, Gutzwiller JP, Beglinger C, Drewe J. Mapping of multidrug resistance gene 1 and multidrug resistance-associated protein

isoform 1 to 5 mRNA expression along the human intestinal tract. Drug Metab Dispos 2005; 33:219-24. https://doi:10.1124/dmd.104.001354

[2] Estudante M, Morais J, Soveral G, Benet L. Intestinal drug transporters: an overview. Adv Drug Deliv Rev 2013; 65:1340–56 https://doi.org/10.1016/j.addr.2012.09.042

[3] Zhang Y, Benet LZ The gut as a barrier to drug absorption: combined role of cytochrome P450 3A and P-glycoprotein Clin Pharmacokinet 2001; 40:159-68. https://doi:10.2165/00003088-200140030-00002

[4] Murakami T, Bodor E, Bodor N. Modulation of expression/function of intestinal P-glycoprotein under disease states. Expert Opin Drug Metab Toxicol 2020; 16:59-78. https://doi:10.1080/17425255.2020.1701653

[5] Sugioka N, Haraya K, Fukushima K, Ito Y, Takada K. Effects of obesity induced by high-fat diet on the pharmacokinetics of nelfinavir, a HIV protease inhibitor, in laboratory rats. Biopharm Drug Dispos 2009; 30:532–41. https://doi.org/10.1002/bdd.689

[6] Watanabe M, Kobayashi M, Ogura J, Takahashi N, Yamaguchi H, Iseki K. Alteration of pharmacokinetics of grepafloxacin in type 2 diabetic rats. J Pharm Pharm Sci 2014; 17:25–33. https://doi.org/10.18433/j3mc70

[7] Grundy SM. Metabolic syndrome pandemic. Arterioscler Thromb Vasc Biol 2008; 28:629-36. https://doi:10.1161/ATVBAHA.107.151092

[8] Esser N, Legrand-Poels S, Piette J, Scheen AJ, Paquot N. Inflammation as a link between obesity, metabolic syndrome and type 2 diabetes. Diabetes Res Clin Pract 2014; 105:141-50. https://doi: 10.1016/j.diabres.2014.04.006

[9] Rogero M, Calder PC. Obesity, Inflammation, Toll-Like Receptor 4 and Fatty Acids. Nutrients 2018; 10:432. https://doi:10.3390/nu10040432

[10] Nigam SK. What do drug transporters really do? Nat Rev Drug Discov 2015; 14:29-44. https://doi:10.1038/nrd4461

[11] Daryabor G, Kabelitz D, Kalantardoi K. An update on immune dysregulation in obesity-related insulin resistance. Scand J Immunol 2019; 89:e12747; https://doi:10.1111/sji.12747

[12] Hotamisligil GS, Shargill NS, Spiegelman BM. Adipose expression of tumor necrosis factor-alpha: direct role in obesity-linked insulin resistance. Science 1993; 259:87-91. https://doi:10.1126/science.7678183

[13] Hotamisligil GS, Arner P, Caro JF, Atkinson RL, Spiegelman BM. Increased adipose tissue expression of tumor necrosis factor-alpha in human obesity and insulin resistance. J Clin Invest 1995; 95:2409-15. https://doi:10.1172/JCI117936

[14] Ding S, Chi MM, Scull BP, Rigby R, Schwerbrock NMJ, Magness S, et al. High-fat diet: bacteria interactions promote intestinal inflammation which precedes and correlates with obesity and insulin resistance in mouse. PLoS One 2010; 5:e12191. https://doi:10.1371/journal.pone.0012191

[15] Wandrer F, Liebig S, Marhenke S, Vogel A, John K, Manns MP, et al. TNF-Receptor-1 inhibition reduces liver steatosis, hepatocellular injury and fibrosis in NAFLD mice. Cell Death Dis 2020; 11:212. https://doi:10.1038/s41419-020-2411-6

[16] Feng Y, Teitelbaum DH. Tumour necrosis factor--induced loss of intestinal barrier function requires TNFR1 and TNFR2 signalling in a mouse model of total parenteral nutrition. J Physiol 2013; 591:3709-23. https://doi:10.1113/jphysiol.2013.253518

[17] Lambertucci F, Arboatti A, Sedlmeier MG, Motiño O, Alvarez ML, Ceballos MD, et al. Disruption of tumor necrosis factor alpha receptor 1 signaling accelerates NAFLD progression in mice upon a high-fat diet. J Nutr Biochem 2018; 58:17-27. https://doi:10.1016/j.jnutbio.2018.04.013

[18] Nawa A, Fujita-Hamabe W, Tokuyama S. Altered intestinal P-glycoprotein expression levels in a monosodium glutamate-induced obese mouse model. Life Sci 2011; 89:834–38. https://doi:10.1016/j.lfs.2011.08.019

[19] Lu X, Dong Y, Jian Z, Li Q, Gong L, Tang L, et al. Systematic investigation of the effects of long-term administration of a high-fat diet on drug transporters in the mouse liver, kidney and intestine. Curr Drug Metab 2019; 20:742-55. https://doi: 10.2174/1389200220666190902125435

[20] Kawase A, Norikane S, Okada A, Adachi M, Kato Y, Iwaki M. Distinct alterations in ATP-binding cassette transporter expression in liver, kidney, small intestine, and brain in adjuvant-induced arthritic rats. J Pharm Sci 2014; 103:2556-64. https://doi: 10.1002/jps.24043

[21] Sukhai M, Yong A, Pak A, Piquette-Miller M. Decreased expression of P-glycoprotein in interleukin-1beta and interleukin-6 treated rat hepatocytes. Inflam Res 2001; 50:362–70. https://doi:10.1007/PL00000257

[22] Lee G, Piquette-Miller M. Cytokines alter the expression and activity of the multidrug resistance transporters in human hepatoma cell lines; analysis using RT-PCR and cDNA microarrays J Pharm Sci. 2003; 92:2152-63. https://doi:10.1002/jps.10493

[23] Evseenko DA, Paxton JW, Keelan JA. Independent regulation of apical and basolateral drug transporter expression and function in placental trophoblasts by cytokines, steroids, and growth factors. Drug Metab Dispos. 2007; 35:595-01. https://doi:10.1124/dmd.106.011478

[24] Collins S, Martin TL, Surwit RS, Robidoux J. Genetic vulnerability to diet-induced obesity in the C57BL/6J mouse: physiological and molecular characteristics. Physiol Behav 2004; 81:243-8. https://doi:10.1016/j.physbeh.2004.02.006

[25] Petro AE, Cotter J, Cooper DA, Peters JC, Surwit SJ, Surwit RS. Fat, carbohydrate, and calories in the development of diabetes and obesity in the C57BL/6J mouse. Metabolism 2004; 53:454-7. https://doi:10.1016/j.metabol.2003.11.018

[26] Londero AS, Arana MR, Perdomo VG, Tocchetti GN, Zecchinati F, Ghanem CI, et al. Intestinal multi drug resistance-associated protein 2 is down-regulated in fructose-fed rats. J Nutr Biochem. 2017; 40:178-86. https://doi:10.1016/j.jnutbio.2016.11.002

[27] Zecchinati F, Barranco MM, Arana MR, Tocchetti GN, Domínguez CJ, Perdomo VG, et al. Reversion of down-regulation of intestinal multidrug resistance associated protein 2 in fructose-fed rats by geraniol and vitamin C. Potential role of inflammatory response and oxidative stress. The Journal of Nutritional Biochemistry 2019; 68:7-15. https://doi:10.1016/j.jnutbio.2019.03.002

[28] Marinho R, Pereira de Moura L, Almeida Rodrigues B, Santos Souza Pauli L, Sanchez Ramos da Silva A, Chiarreotto Ropelle EC et al. Effects of different intensities of physical exercise on insulin sensitivity and protein kinase B/Akt activity in skeletal muscle of obese mice. Einstein (Sao Paulo) 2014; 12:82-9. https://doi:10.1590/S1679-45082014AO2881

[29] Falcato Vecina J, Gabarra Oliveira A, Gomes Araujo T, Regina Baggio S, Okuda Torello C, Abdalla Saad MJ, et al. Chlorella modulates insulin signaling pathway and prevents high-fat diet-induced insulin resistance in mice. Life Sciences 2014; 95:45–52. https://doi:10.1016/j.lfs.2013.11.020

[30] Ohkura T, Yoshimura T, Fujisawa M, Ohara T, Marutani R, Usami K, et al. Spred2 regulates high fat diet-induced adipose tissue inflammation, and metabolic abnormalities in mice. Front Immunol 2019; 10-7. https://doi:10.3389/fimmu.2019.00017

[31] Villanueva SSM, Arias A, Ruiz ML, Rigalli JP, Pellegrino JM, Vore M, et al. Induction of intestinal multidrug resistance-associated protein 2 by glucagon-like

Peptide 2 in the rat. J Pharmacol Exp Ther 2010; 335:332-41. https://doi:10.1124/jpet.110.171041

[32] Yan S, Khambu B, Chen X, Dong Z, Guo G, Yin XM. Hepatic autophagy deficiency remodels gut microbiota for adaptive protection via FGF15-FGFR4 signaling. Cellular and Molecular Gastroenterology and Hepatology 2021;11:973-97. https://doi.org/10.1016/j.jcmgh.2020.10.011

[33] Lee JY, Mori C, Tokumoto M, Satoh M. Time-dependent changes in the gene expression levels in the mouse kidney by long-term exposure to cadmium. BPB Reports 2021; 4:69-73. https://doi.org/10.1248/bpbreports.4.2_69

[34] Cribb P, Perdomo V, Alonso VL, Manarin R, Barios-Payán J, Marquina-Castillo B, et al. *Trypanosoma cruzi* High Mobility Group B (*Tc* HMGB) can act as an inflammatory mediator on mammalian cells. PloS Negl Trop Dis 2017; 11:e0005350. https://doi:10.1371/journal.pntd.0005350

[35] Livak KJ, Schmittgen TD. Analysis of relative gene expression data using real-time quantitative PCR and the 2(-Delta Delta C(T)) Method. Methods. 2001; 25:402–08.

[36] Mottino AD, Hoffman T, Jennes L, Vore M. Expression and localization of multidrug resistant protein mrp2 in rat small intestine. J Pharmacol Exp Ther 2000; 293:717-23

[37] Guo M, Bughio S, Sun Y, Zhang Y, Dong L, Dai X, Wang L. Age-Related P glycoprotein expression in the intestine and affecting the pharmacokinetics of orally administered enrofloxacin in broilers. PLoS ONE 2013; 8: e74150. https://doi:10.1371/journal.pone.0074150

[38] Arana MR, Tochetti GN, Zecchinati F, Londero AS, Dominguez C, Perdomo V, et al. Glucagon-like peptide 2 prevents down-regulation of intestinal multidrug resistance-associated protein 2 and P-glycoprotein in endotoxemic rats. Toxicology 2017; 39:22–31. https://doi.org/10.1016/j.tox.2017.08.007

[39] Lowry OH, Rosebrough NJ, Farr AL, Randall RJ. Protein measurement with the Folin phenol reagent. J Biol Chem 1951; 193:265-75.

[40] Chianale J, Vollrath V, Wielandt AM, Miranda S, Gonzalez R, Fresno AM, et al. Differences between nuclear run-off and mRNA levels for multidrug resistance gene expression in the cephalocaudal axis of the mouse intestine**.** Biochim. Biophys. Acta 1995, 1264: 369-76. https://doi.org/10.1016/0167-4781(95)00179-4

[41] Bhering Martins L, Chaves de Oliveira M, Menezes-Garcia Z, Fernandes D. Paradoxical role of tumor necrosis factor on metabolic dysfunction and adipose tissue expansion in mice. Nutrition 2018; 50:1-7. https://doi: 10.1016/j.nut.2017.07.006

[42] Darwich AS, Neuhoff S, Jamei M, Rostami-Hodjegan A. Interplay of metabolism and transport in determining oral drug absorption and gut wall metabolism: a simulation assessment using the "Advanced Dissolution Absorption, Metabolism (ADAM)": model. Curr Drug Metab 2010; 11:716–29. https://doi:10.2174/138920010794328913

[43] Wang Z, Yang H, Xu J, Zhao K, Chen Y, Liang L, et al. Prediction of Atorvastatin Pharmacokinetics in High-Fat Diet and Low-Dose Streptozotocin-Induced Diabetic Rats Using a Semiphysiologically Based Pharmacokinetic Model Involving Both Enzymes and Transporters Drug Metab Dispos 2019; 47:1066-79. https://doi:10.1124/dmd.118.085902

[44] Nawa A, Fujita-Hamabe W, Tokuyama S. Inducible nitric oxide synthase-mediated decrease of intestinal P-glycoprotein expression under streptozotocin-induced diabetic conditions. Life Sciences 2010; 86: 402–09. https://doi:10.1016/j.lfs.2010.01.009

[45] Belliard AM, Lacour B, Farinotti R, Leroy C. Effect of tumor necrosis factor-alpha and interferon-gamma on intestinal P-glycoprotein expression, activity, and localization in Caco-2 cells. J Pharm Sci 2004; 93:1524-36. https://doi:10.1002/jps.20072

[46] Walther W, Kobelt D, Bauer L, Aumann J, Stein Ulrike Chemosensitization by diverging modulation by short-term and long-term TNF-α action on ABCB1 expression and NF-κB signaling in colon cancer Int J Oncol. 2015; 47:2276-85. . https://doi: 10.3892/ijo.2015.3189.

[47] Williams JM, Duckworth CA, Watson AJM, Frey MR, Miguel JC, Burkitt MD, et al. A mouse model of pathological small intestinal epithelial cell apoptosis and shedding induced by systemic administration of lipopolysaccharide. Dis Model Mech 2013; 6:1388-99. https://doi:10.1242/dmm.013284

CRediT authorship contribution statement

María Manuela Barranco: Surgery and animal treatment, Methodology, Investigation, Formal analysis, Writing - Original Draft.

Virginia Gabriela Perdomo: Surgery and animal treatment, Methodology, Investigation, Formal analysis, Software and Figures preparations.

Felipe Zecchinati: Surgery, Methodology, Formal analysis, Investigation.

Romina Manarin and Silvana Vignaduzzo: Methodology

Greta Massuh and Nicolás Sigal: Surgery and animal treatment

Aldo Domingo Mottino: Critical Revision and Funding acquisition.

Silvina Stella Maris Villanueva and Fabiana García: Conceptualization, Funding acquisition, Supervision, Data Curation, Writing Original Draft, Project administration. Writing - review & editing

All authors: Approved the final form

Declaration of interests

☒ The authors declare that they have no known competing financial interests or personal relationships that could have appeared to influence the work reported in this paper.

☐The authors declare the following financial interests/personal relationships which may be considered as potential competing interests: